Liquefaction assessment at gravel sites in Croatia based on V_s and DPT blow count

Kyle Rollins[1], *Sara* Amoroso[2,3], *Alicia* Walburger[1], *Giuseppe* di Giulio[3], *Nikola* Belić[4], *Kosta* Urumović[4], *Radovan* Filjak[4], *Luca* Minarelli[3], *Gabriele* Tarabusi[5], *Davor* Stanko[6,7], *Snježana* Markušić[7], *Lorena* Marenghi[8] and *Maurizio* Vassallo[3]

[1]*Brigham Young University, Dept. of Civil and Construction Engineering, Provo UT, USA*
[2]*Univ. of Chieti-Pescara, Dept. of Engineering and Geology, Pescara, Italy*
[3]*INGV Istituto Nazionale di Geofisica e Vulcanologia, L'Aquila, Italy*
[4]*Croatian Geological Survey, Dept. of Geology, Zagreb, Croatia*
[5]*INGV Istituto Nazionale di Geofisica e Vulcanologia, Bologna, Italy*
[6]*Univ. of Zagreb, Faculty of Geotechnical Engineering, Varaždin, Croatia*
[7]*Univ. of Zagreb, Faculty of Science, Dept. of Geophysics, Zagreb, Croatia*
[8]*Univ. of Modena and Reggio-Emilia, Dept. of Chemical and Geological Sciences, Modena, Italy*
[1]*Corresponding author: rollinsk@byu.edu*

ABSTRACT

Liquefaction of loose saturated soil poses a significant threat to civil infrastructure during major earthquake events. Although liquefaction is most common in loose saturated sands, numerous liquefaction events in gravelly soil profiles have been reported. Assessing liquefaction resistance in gravelly soils is challenging because large particle sizes can interfere with the standard penetration test (SPT) and the cone penetration test (CPT). To address this challenge, recent efforts have focused on developing liquefaction triggering curves based on a large diameter (74 mm) dynamic cone penetrometer (DPT) blow count and normalized shear wave velocity, V_{s1}, which are less affected by gravel-sized particles. While based on field case histories, the curves are poorly constrained in some areas; additional case histories continue to be highly desirable. This paper describes an investigation of six gravel sites that liquefied in the 2020 M_w6.4, Petrinja, Croatia earthquake. At each site, boreholes were completed to define the soil profile, accompanied by DPT soundings and shear wave velocity profiling using the Multi-channel Analysis of Surface Waves (MASW) approach. At some sites, the DPT blow count increased through a silty clay surface layer even though the CPT cone resistance remained constant in this layer. This increase was thus attributed to side friction on the drill rods during penetration. Subsequent DPT tests performed after casing through the silty clay eliminated the rod friction. The measured blow count and shear wave velocities in the critical layers at these sites correctly predicted liquefaction using recent probabilistic DPT- and V_{s1}-based triggering curves.

Keywords: Gravel liquefaction; Dynamic Cone Penetration Test (DPT); Shear wave velocity; Croatia earthquake.

1. Introduction

Finding a reliable and economical way to characterize gravelly soil and assess its susceptibility to liquefaction is a current challenge in geotechnical engineering. In the past 130 years, the liquefaction of gravelly soils has occurred at a significant number of earthquake sites (Rollins et al. 2021). The damage associated with gravel liquefaction in these events is significant and reinforces the need to find a more efficient and accessible method for identifying gravelly soils prone to liquefaction.

An in-situ test such as the standard penetration test (SPT) or a cone penetration test (CPT) would be preferable for performing a liquefaction analysis. However, these methods are not commonly used in gravelly material due to interference with the large particles. With a large particle size to penetrometer diameter ratio, CPT and SPT performed in gravelly material may show an increase in penetration resistance even when the density of the material is relatively low or remains constant (Daniel et al. 2004).

An in-situ test for gravelly soils, developed in China, is the dynamic cone penetration test (DPT). The Chinese DPT consists of a 74 mm diameter cone, driven continuously by a 120 kg hammer dropped from a free-fall height of 100 cm. With a cone tip diameter of 74 mm, the DPT is 110% larger than a standard 10 cm^2 CPT and 50% larger than the SPT. The DPT cone also tapers from a 74 mm diameter to a 60 mm diameter drill rod to reduce rod friction.

The DPT has been used by Chinese engineers over the past 60 years to effectively penetrate coarse or cobbly gravels and collect penetration data useful for foundation design (Chinese Design Code 2001). The penetration resistance from the Chinese DPT was correlated with liquefaction resistance by Cao et al. (2013) based on 47 DPT soundings from 19 sites with liquefaction effects and 28 sites without liquefaction from the 2008 M_w 7.9 Wenchuan earthquake. The triggering curves were later updated by Rollins et al. (2021) using an expanded data set of 137 sites from 10 earthquakes in seven countries where liquefaction did or did not occur. This update led to notable adjustments in the liquefaction triggering curves, reemphasizing the importance of collecting additional field data to more accurately define and adjust the triggering curves as necessary.

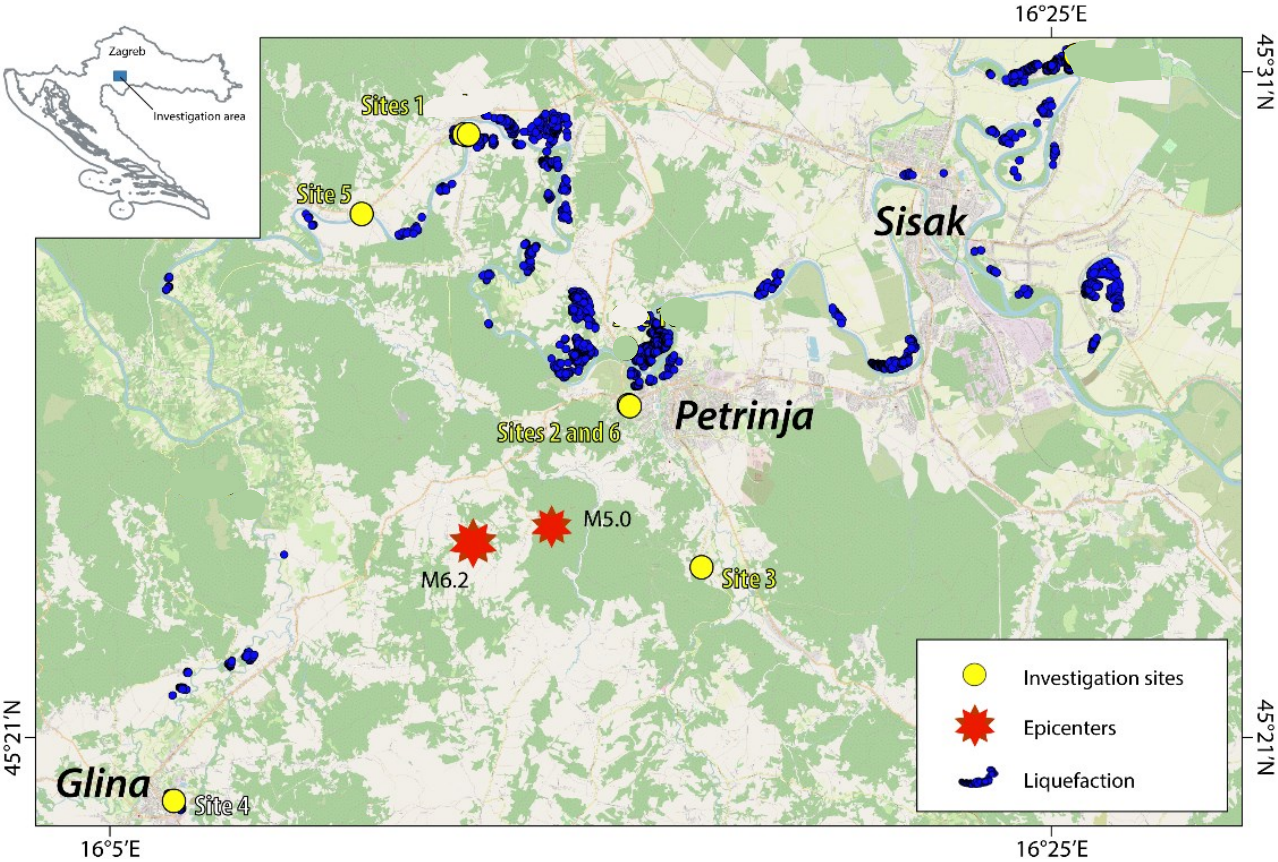

Figure 1. Base map (OpenStreetMap WMS Service) with location of investigation sites, 2020 earthquake epicenters (Baize et al. 2022) and liquefaction features from the HGI drone and available satellite images (Amoroso et al. 2023).

An alternative to penetration testing is liquefaction triggering curves based on the shear wave velocity, V_s. This method is often performed using surface wave methods and eliminates the need for a borehole and the associated interference with large particles. V_s-based liquefaction triggering curves have been developed for gravel specifically by Cao et al. (2011) and Chang (2016) but have been updated with much more field data by Rollins et al. (2022).

This study includes an investigation of six gravel sites in Croatia that liquefied in the 2020 M_w6.4, Petrinja, Croatia earthquake (see Fig. 1), as reported by Amoroso et al. (2023). At each site, a borehole was completed to define the soil profile and material properties, and at Sites 1 and 5, a CPT was also performed. In addition, a DPT sounding was performed at each site along with shear wave velocity profiling using the Multi-channel Analysis of Surface Waves (MASW) approach using both active and passive methods.

At some sites, the DPT blow count increased as the penetrometer passed through a clayey silt surface layer even though the associated CPT cone resistance remained constant in this layer. This increase was thus attributed to side friction on the drill rods during penetration. Subsequent DPT tests were performed at Sites 1 and 5 after casing through the silty clay to eliminate the rod friction and provide appropriate blow counts. This paper considers the results from Sites 1 and 5 specifically to: (1) investigate the use of casing and the influence of rod friction during these DPT soundings, (2) examine the applicability of the recently developed DPT- and V_s-based liquefaction triggering methods for the evaluation of liquefaction potential in gravelly soils, and (3) to expand the database of DPT and V_s case histories in gravelly soils to assist in the development of improved predictive models in the future.

2. Geologic Setting and Liquefaction Effects

The Petrinja earthquake affected the southwestern margin of the Sava Basin in the Pannonian Basin System in the continental part of Croatia (Pollak et al. 2021) shown in Fig. 1. During the Tertiary, the region was subjected to tectonic extension and compression to eventually generate a complex framework of NW-SE striking, inverted normal faults (Tomljenović and Csontos 2001, Ustaszewski et al. 2010). The epicentral area of the 29th December 2020 earthquake is in the Hrastovička mountains, composed of various basement rocks (Jurassic-Paleogene) (Šikić 2014). Most of the seismic effects recorded were in the alluvial plains of the Glina, Kupa, and Sava rivers. The affected sediments were deposited in different environments such as flood plains, meander oxbows, and active streams. The liquefaction affected lithologies vary widely from clays, to silts, sands, and gravels with silt layers predominating at the surface (Baize et al. 2022).

The Petrinja earthquake source is associated with the Petrinja-Pokupsko Fault (PPKF). The liquefaction phenomena occurred in the lowlands at elevations between 100 and 200 meters as shown in Fig. 1. Some of the observations from the field reconnaissance campaigns following the earthquake include liquefaction on alluvial plain sites along the Kupa, Sava, and Glina rivers; sand and/or gravel ejecta with shells and armored mud balls, lateral spreading along roads and river embankments, and sand and/or gravel ejecta along fault traces (Amoroso et al. 2023).

3. DPT Testing and Interpretation

3.1. DPT corrected blow count (*N'₁₂₀*)

As part of this study, DPT soundings were performed at 6 different locations where gravel liquified during the Croatia earthquake. Due to observed rod friction through a clayey silt surface layer at some of the sites, subsequent DPT soundings at Sites 1 and 5 used casing to eliminate rod friction through the clayey silt layer. The DPT tests were performed using a standard Chinese DPT consisting of a 74 mm cone tip, 60 mm drill rod, and a 63.5 kg hammer dropped from a free-fall height of 76 cm (See Fig. 2). Prior to testing, the drill rods are marked at 10 cm intervals and the number of blows required to penetrate each 10 cm is recorded. The raw DPT blow count is defined as the number of hammer drops required to advance the cone tip 10 cm. A second penetration resistance measure, called N_{120}, is the number of blows required to drive the cone tip 30 cm; however, N_{120} is calculated simply by multiplying raw blow counts by a factor of three which preserves the detail of the raw blow count record.

Hammer energy measurements were collected during the DPT soundings using a Pile Driving Analyzer (PDA) device from PDI Inc. A correction for the difference between applied hammer energy and theoretical hammer energy was made using the following equation suggested by Seed et al. (1985) for SPT testing:

$$N_{120} = N_{Measured} \frac{E_{Delivered}}{E_{ChineseDPT}} \quad (1)$$

where $N_{Delivered}$ is the number of blows per 30 cm of penetration obtained while using a hammer delivering an energy of $E_{Delivered}$. Based on 1200 energy measurements collected by Cao et al. (2013), the $E_{ChineseDPT}$ is 89% of the theoretical free-fall energy equal to a 120 kg hammer dropped from a free-fall height of 100 cm. In this study, the delivered hammer energy ($E_{Delivered}$) is the theoretical standard SPT hammer energy times the hammer efficiency (89% for Sites 1 and 5). The ratio of hammer energy delivered, divided by the energy delivered by the Chinese DPT hammer was 0.4 for both Site 1 and Site 5.

An additional correction for overburden stress on the DPT blow count is applied using the equation:

$$N'_{120} = N_{120} C_N; \; C_N = \sqrt{100/\sigma'_{vo}} \leq 1.7 \quad (2)$$

where N'_{120} is the corrected DPT resistance in blows per 30 cm, 100 is atmospheric pressure in kN/m^2, and σ'_{vo} is the vertical effective stress in kN/m^2. A limiting value of 1.7 was added to be consistent with the C_N used in other in-situ test methods (Rollins et al. 2021). Blow counts recorded at Sites 1 and 5 during the uncased and cased DPT soundings were corrected accordingly and plotted versus depth as shown in Fig. 3. The difference in N'_{120} values from the uncased and cased DPT soundings along with the consistent CPT tip resistance values suggest that rod friction did artificially increase the DPT blow counts recorded from the uncased hole as suggested by Amoroso et al. (2023).

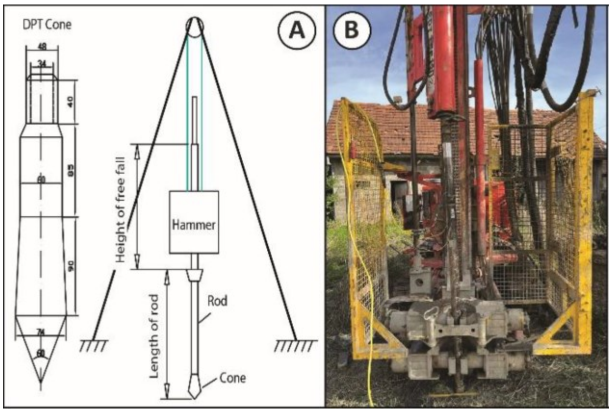

Figure 2. (a) Component sketch of tripod and drop hammer setup for dynamic penetration tests (DPT) along with DPT cone tip; (b) photo of DPT testing at one of the Croatian site investigations with conventional drill rig (Amoroso et al. 2023).

3.2. DPT rod friction

The Chinese DPT reduces rod friction by connecting the 74 mm DPT cone to a 60 mm diameter drill rod. Chinese experience expects rod friction in soft clays or at depths greater than 20 m. Cao et. al (2013) suggested that in such conditions, the borehole should be cased. However, it has been noted in multiple succeeding studies that further investigation considering the effect of rod friction would be beneficial. Measurements are necessary to understand how the hammer energy transferred to the drill rods varies with depth and any possible limitations associated with the DPT due to rod friction (Rollins et al. 2021). The surface layers creating rod friction at some of the Croatia sites vary in percent clay, silt, and sand, and were less than 20 m below the surface; therefore, rod friction was not anticipated. Nevertheless, results from both the initial, uncased, DPT soundings and the subsequent cased DPT soundings affirm the need to obtain better understanding regarding drill rod friction. Further investigations concerning rod friction and methods for quantifying the reduction in energy transferred to the drill rods with depth are underway.

3.3. Liquefaction resistance based on DPT-penetration resistance

The probabilistic liquefaction triggering curves recently developed by Rollins et. al (2021) based on DPT resistance in gravelly soils are based on the corrected N'_{120} blow counts and the associated cyclic stress ratio (CSR) for the critical layer at gravel sites that did and did not liquefy in past earthquakes. The CSR for a M_w7.5 earthquake, ($CSR_{M=7.5}$) is given by the equation:

$$CSR_{M=7.5} = 0.65 \frac{a_{max}}{g} \frac{\sigma_{v0}}{\sigma'_{v0}} r_d \frac{1}{MSF} \quad (3)$$

where a_{max} is the peak ground acceleration in g's, g is the acceleration of gravity, σ_{vo} and σ'_{vo} are total and effective vertical stress at a given depth, r_d is a factor account for flexibility of the soil profile, and MSF is the magnitude scaling factor that adjusts the CSR to a 7.5 magnitude.
For DPT-based liquefaction assessment, MSF is given by the equation:

$$MSF = 7.258 \exp(-0.264 M_w) \quad (4)$$

where M_w is the moment magnitude of the earthquake.

Following the DPT-based procedure outlined by Rollins et. al (2021), the DPT-based $CSR_{M=7.5}$ and cyclic resistance ratio (CRR) curves were developed and plotted versus depth for Sites 1 and 5, as shown in Fig 4. Because ground motion recordings were not available, the a_{max} values were estimated using prediction equations developed by Uglešić et al. (2022) which include the V_s values at each site. The CRR curves were calculated based on a 15% probability of liquefaction. At depths where the $CSR_{M=7.5}$ exceeds the CRR, there is likely to be liquefaction. The critical liquefaction layer, at least 1 m thick, was selected from the cased test using the lowest average N'_{120} value in gravelly soil below the water table.

The DPT-based critical layer at Site 1 was located at a depth of 10 m with a measured 48% gravel content, 39% sand content, and 13% fines content, and an estimated hydraulic conductivity of $7.01*10^{-6}$ m/sec. The N'_{120} critical layer at Site 5 was located at a depth of 11 m with a measured 56% gravel content, 41% sand content, and 3% fines content, and an estimated hydraulic conductivity of $3.46*10^{-4}$ m/sec. Therefore, the critical layer of the sandy-gravelly mixture at both the sites will likely behave as a sand in terms of permeability and pore pressure generation (Roy 2023, Chang et al. 2014). A summary of each site and its critical layer properties is shown in Table 1.

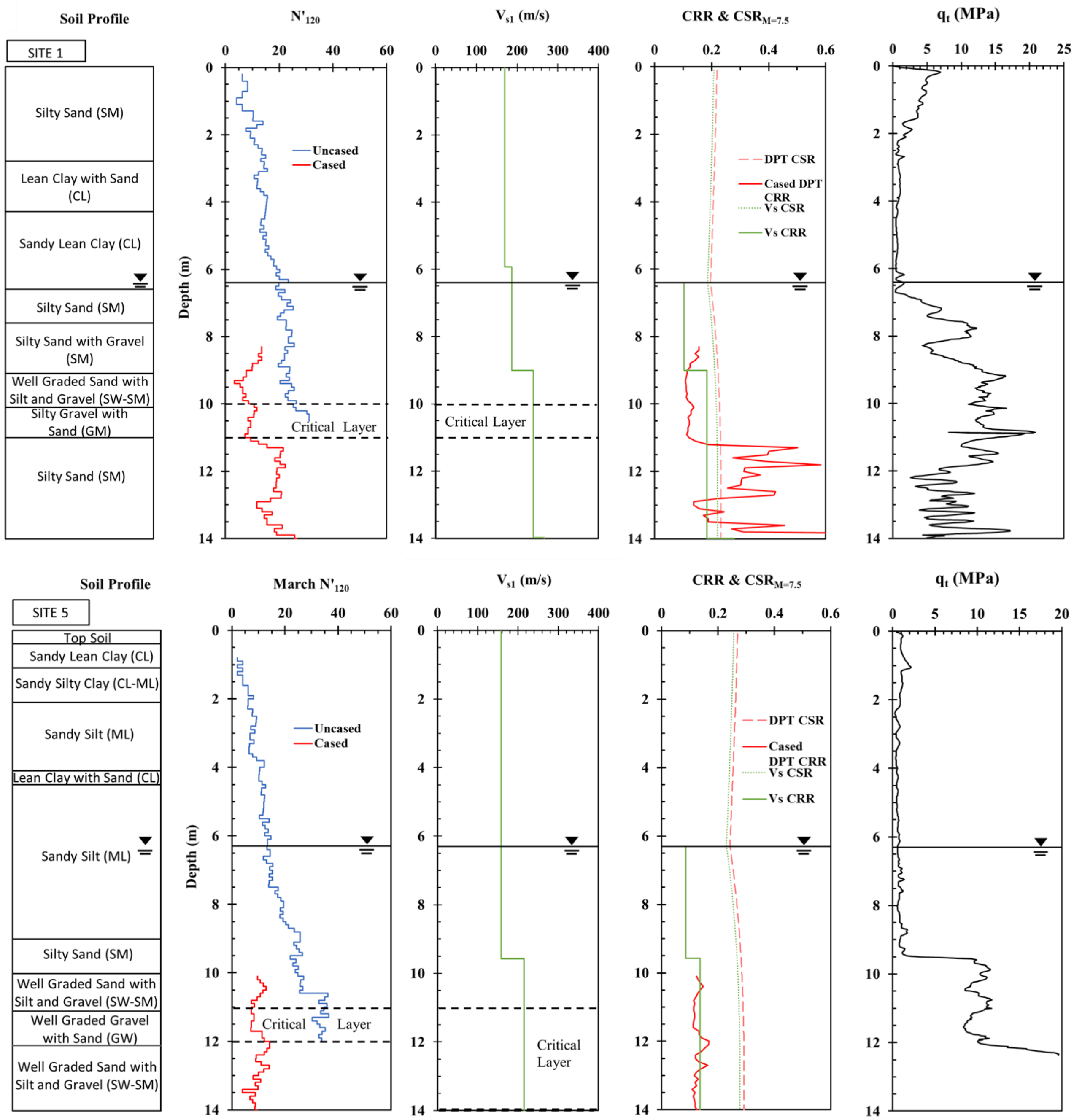

Figure 3. Corrected DPT blow counts, Vs1, CRR, CSRM=7.5, and CPT cone resistance at Site 1 and Site 5.

4. MASW Testing and Interpretation

As part of this study, shear wave velocity (V_s) profiles were developed using the Multi-channel Analysis of Surface Waves (MASW) approach near each DPT site. Both active and passive methods were employed in these investigations (Parks et al. 2007). Active MASW surveys were performed using a linear array of geophones with a maximum of 72 vertical 4.5 Hz geophones connected to a multi-channel acquisition system manufactured by Geometrics. Files were recorded in 1.5s increments with a sampling rate of 8000 Hz. The geophones were equally spaced 1 m at Site 1 and 0.5 m at Site 5. The linear array recorded seismic signals produced by striking a metal plate located at the beginning, middle, and end of the linear array with a 5 kg sledgehammer to reproduce forward and reverse shot records The MASW technique uses these records to retrieve the Rayleigh and Love wave dispersion curves needed to develop the V_s profiles (Amoroso et al. 2023). For the passive surveys, 2D arrays were employed with 20 to 46 nodes. Seismic nodes were arranged at each site in a circular geometry with typically three circular rings of different radii (about 5, 12 and 25 m), and a node in the center, close to the DPT sounding (see Fig. 4). These seismic nodes recorded ambient vibrations at each site for a few hours with a sampling rate of 250 Hz. Seismic noise data were used to compute the horizontal-to-vertical noise spectral ratio (H/V curve) and then to derive the site resonance frequency (f0), important in site characterization and microzoning activities, for detecting the presence of a seismic contrast in the subsoil profile (Di Giulio et al. 2021). Results from both arrays were then used jointly to perform the inversions and define the shear wave velocity profile versus depth (Parks et al. 2007).

The V_s values were corrected for overburden pressure to obtain normalized shear wave velocity (V_{s1}) using the following equation:

$$V_{s1} = V_s(P_a/\sigma'_{vo})^{0.25} \qquad (5)$$

where P_a is atmospheric pressure approximated by a value of 100 kPa, and σ'_{vo} is the initial vertical effective stress at the center of each layer to preserve the constant velocity assumed in the MASW interpretation process (Rollins et al. 2022). The correction coefficient is limited to a value of 1.4 based on personal communication with Roy (2024). The normalized V_{s1} profiles from Sites 1 and 5 are plotted versus depth as shown in Fig. 3.

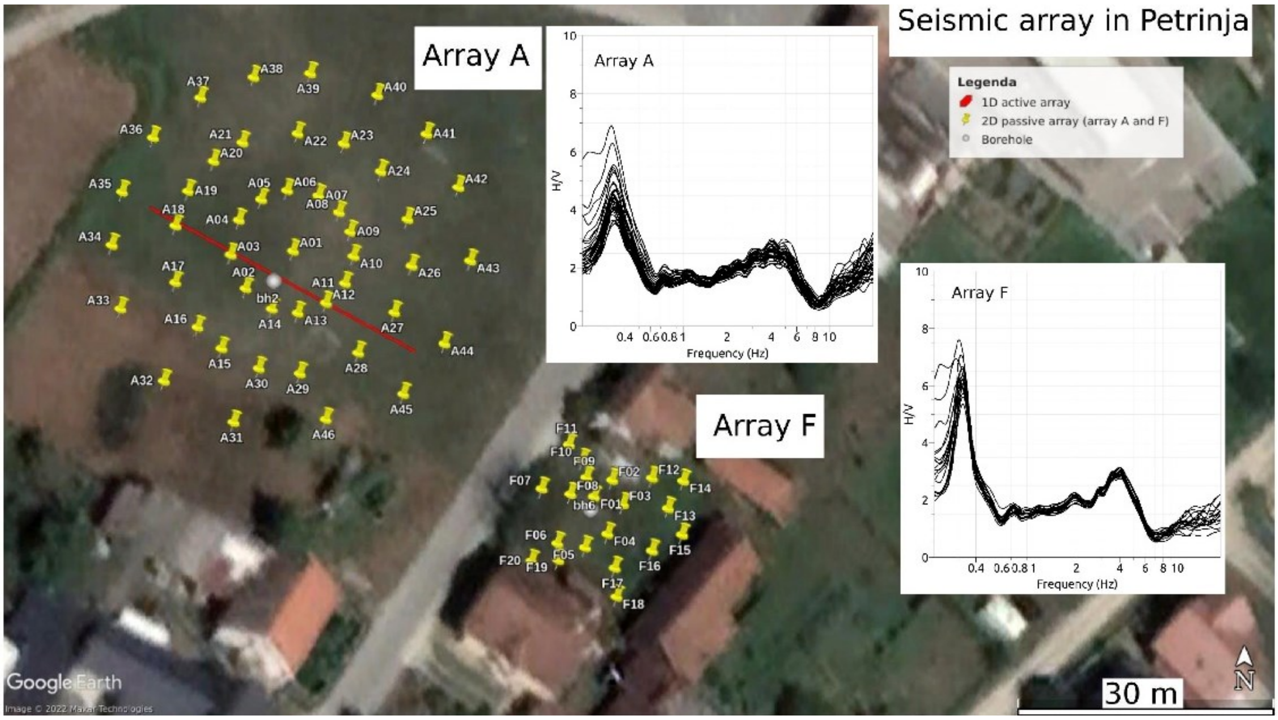

Figure 4. Seismic array configurations and mean H/V curves in Petrinja (Amoroso et al. 2023

4.1. Liquefaction resistance based on normalized shear wave velocity

Liquefaction triggering curves for gravelly soils based on V_{s1} were initially developed by Cao et al. (2011) based on gravel liquefaction case histories from the 2008 M_w7.9 Wenchuan earthquake. Subsequently, triggering curves developed by Rollins et al. (2022) using a world-wide earthquake data set along with the Wenchuan earthquake data to refine the triggering curves. This study uses the recent triggering curves to evaluate the liquefaction potential of gravelly soils using V_{s1}-based $CSR_{M=7.5}$ and CRR versus depth at Site 1 and Site 5 in Croatia (See Fig. 3).

For the V_{s1}-based approach, CRR curves were calculated based on a 15% probability of liquefaction, and Eq. 3 was also used for CSR except that the MSF was based on the value specifically derived from the shear wave data given by:

$$MSF = 10.667\exp(-0.316M_w) \qquad (6)$$

In the liquefaction analysis, the V_{s1}-based critical layer was selected as the gravelly layer with the lowest average V_{s1} below the water table most likely to liquefy. As with the DPT approach, the critical V_{s1} layer selected was at least 1 m thick to minimize the effect of local variations (Rollins et al. 2022). The V_{s1}-based critical layer and the DPT-based critical layer are generally located at similar depths but may vary depending on testing procedures and results. In this study, the critical layer selected at Site 1 using the V_{s1}-based approach was 10 m below the surface with a measured 48% gravel content, 39% sand content, and 13% fines content, and an estimated hydraulic conductivity of $7.01*10^{-6}$ m/sec. The V_{s1}-based critical layer at Site 5 started 11 m below the surface with average measured soil gradation properties of 47% gravel, 49% sand, and 4% fines, and an estimated average hydraulic conductivity of $3.42*10^{-4}$ m/sec (see Table 1). Therefore, the critical layer of the sandy-gravelly mixture at both the sites will likely behave as a sand in terms of permeability and pore pressure generation (Roy 2023, Chang et al. 2014)..

Table 1. Soil and earthquake parameters for critical layers at Croatia Site 1 and Site 5.

Site	Method	Critical Layer Depth (m)	Critical Layer Thickness (m)	Avg. G.C (%)	Avg. S.C. (%)	Avg. σ_{vo} (kPa)	Avg. σ'_{vo} (kPa)	Avg. N'_{120}	Avg. V_{s1} (m/s)	PGA (g)*	Avg. $CSR_{M=7.5}$	k (m/sec)
1	DPT	10	1	48.1	39.3	174.6	134.4	9.5	-	0.45	0.230	$7.01*10^{-6}$
	V_{s1}	10	1	48.1	39.3	174.6	134.4	-	240.0	0.45	0.218	$7.01*10^{-6}$
5	DPT	11	1	55.8	40.8	187.5	136.5	9.3	-	0.55	0.291	$3.46*10^{-4}$
	V_{s1}	11	3	47.0	48.6	205.1	144.3	-	215.0	0.55	0.277	$3.42*10^{-4}$

5. Comparison with DPT-based and Vs-based liquefaction triggering curves

5.1. DPT-based liquefaction triggering curves

The DPT-based $CSR_{M=7.5}$ and the N'_{120} for the critical layers at Site 1 and Site 5 are plotted in Fig. 5 with the recent probabilistic liquefaction triggering curves developed by Rollins et al. (2021) based on DPT resistance in gravelly soils. The solid stars on the plots represent the cased test analysis for the sites analyzed in this study, with Site 1 in orange and Site 5 in green. The curves correctly predicted liquefaction at Site 1 and Site 5. The N'_{120} and $CSR_{M=7.5}$ values plot above or near the 85% triggering curve, where liquefaction would be expected.

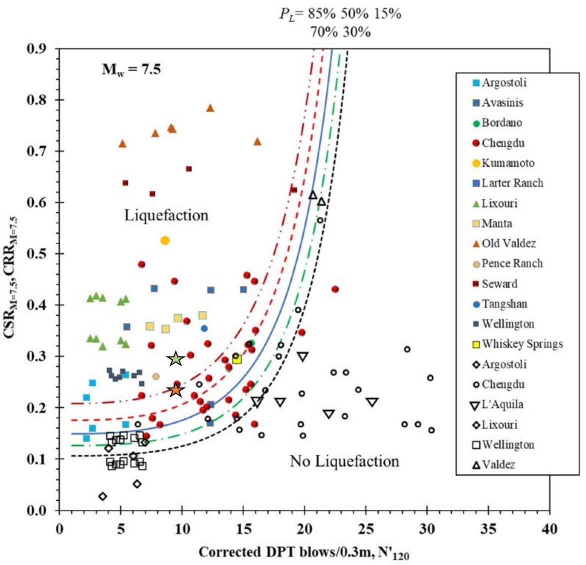

Figure 5. N'_{120} vs. DPT-based $CSR_{M=7.5}$ curves for various probabilities of liquefaction in gravelly soils developed by Rollins et. al (2021) with liquefaction points from 2020 M_w6.4 Croatia earthquake shown as solid star shapes with Site 1 in orange Site 5 in green.

5.2. *V_{s1}* -based liquefaction triggering curves

The V_{s1} and V_{s1}-based $CSR_{M=7.5}$ values for the respective critical layers at Site 1 and Site 5 are plotted in Fig. 6 with the V_{s1}-based liquefaction triggering curves recently developed for gravelly soils (Rollins et al. 2022). The sites from this study are plotted as solid stars with Site 1 in orange and Site 5 in green. Site 5 plots near the 85% triggering curve while Site 1 plots just above the 30% triggering curve.

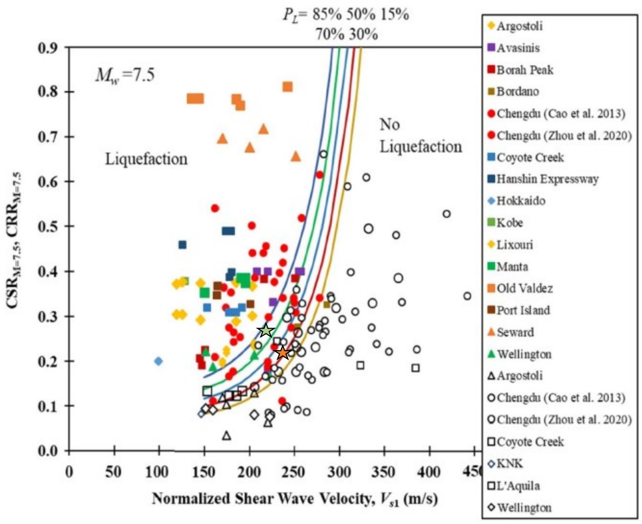

Figure 6. V_{s1} vs. V_{s1} -based $CSR_{M=7.5}$ curves for various probabilities of liquefaction in gravelly soils developed by Rollins et al. (2022) with liquefaction points from 2020 M_w6.4 Croatia earthquake shown as solid star shapes with Site 1 in orange Site 5 in green.

6. Observations and Conclusions

Based on the dynamic cone penetration test (DPT) and shear wave velocity (V_s) investigations conducted in gravelly soils impacted by the 2020 M_w6.4 Petrinja, Croatia earthquake the following observations and conclusions are presented:

1. Rod friction can artificially increase DPT blow counts through saturated clayey silt layers. Casing through the surface layers inducing rod friction is one method for collecting more accurate blow counts in deeper, gravelly layers. Investigations at the gravel sites in Croatia to examine the influence of friction and hammer energy transferred with depth are ongoing.
2. The DPT-based liquefaction triggering curves developed by Rollins et. al (2021) correctly predicted liquefaction at Sites 1 and 5 using the blow counts recorded during the cased DPT sounding and following the new cyclic stress ratio (CSR) procedures. The points from Site 1 and Site 5 lie above the 85% curve, consistent with the liquefaction effects observed in gravel deposits at these sites during the 2020 Croatia earthquake.
3. The V_{s1}-based liquefaction triggering curves developed by Rollins et al. (2022) also correctly predicted liquefaction at Sites 1 and 5. Using the normalized shear wave velocity and V_{s1}-based $CSR_{M=7.5}$ both Sites 1 and 5 plot between the 85%

and 30% probability of liquefaction triggering curves, consistent with the gravel liquefaction effects observed during the 2020 Croatia earthquake.

4. To further refine the DPT and V_s liquefaction triggering curves for gravelly material, it remains highly desirable to continue incorporating additional dynamic cone penetration test (DPT) and shear wave velocity (V_s) field performance case histories into the predictive models. This study provided two additional field histories that could be used in the predictive model. Ongoing investigations quantifying the reduction of hammer energy due to drill rod friction could be used to correct the DPT blow counts at the four remaining sites. This would provide four more case histories for refining future DPT-based liquefaction triggering curves.

Acknowledgements

Funding for this work was provided by Progetti di Ricerca Libera INGV 2021 (Istituto Nazionale di Geofisica e Vulcanologia) “Liquefaction Assessment of Gravelly Deposits (LAGD; 9999.816): historical data analyses and in situ testing at Italian trial sites to develop innovative methods”, by the Geotechnical Extreme Events Reconnaissance (GEER) organization, by Brigham Young University (Provo, Utah) and by the University of Ferrara (Ferrara, Italy). This support is gratefully acknowleged; however, the opinions, conclusions, and recommendations in this paper do not necessarily represent those of the sponsors. The Authors also thank Nicola Sciarra and Gabriele Toro for their support in the geotechnical analyses at the Laboratory of University of Chieti-Pescara and Diana Faieta for her valuable assistance in the Laboratory.

References

Amoroso S., Rollins K.M., Di Giulio G., Wacha L., Urumović K., Faieta D., Filjak R., Fontana D., Lugli S., Manuel M.R., Milana G., Minarelli L., Budić M., Belić N., Kurečić T., Sorić L., Stefani M., Tarabusi G., Vassallo M. 2023. Geotechnical and geophysical tests following the 2020 earthquake-induced liquefaction phenomena. In Proceedings of the 2nd Croatian Conference on Earthquake Engineering - 2CroCEE. Zagreb, Croatia. https://doi.org/10.5592/CO/2CroCEE.2023.21

Baize, S., Amoroso, S., Belić, N., Benedetti, L., Boncio, P., Budić, M. Cinti, F.R., Henriquet, M., Jamšek Rupnik, P., Kordić, B., Markušić, S., Minarelli, L., Pantosti, D., Pucci, S., Špelić, M., Testa, A., Valkaniotis, S., Vukovski, M., Atanackov, J., Barbača, J., Bavec, M., Brajkovič, R., Brčić, V., Caciagli, M., Celarc, B., Civico, R., De Martini, P.M., Filjak, R., Iezzi F., Moulin, A., Kurečić, T., Métois, M., Nappi, R., Novak, A., Novak, M., Pace, B., Palenik, D. and Ricci T. 2022. Environmental effects and seismogenic source characterization of the December 2020 earthquake sequence near Petrinja, Croatia. Geophysical Journal International, 230(2): pp. 1394–1418. https://doi.org/10.1093/gji/ggac123

Cao, Z. Youd, T.L. and Yuan, X. 2011. Gravelly soils that liquefied during 2008 Wenchuan, China Earthquake, Ms=8.0. Soil Dynamics and Earthquake Engineering 31: 1132-1143.

Cao, Z., T. L. Youd and X. Yuan. 2013. "Chinese Dynamic Penetration Test for Liquefaction Evaluation in Gravelly Soils." Journal of Geotechnical and Geoenvironmental Engineering 139(8): 1320-1333.

Chang, W.J., Chang, C.W., and Zeng, J.K. 2014. Liquefaction characteristics of gap-graded gravelly soils in K0 condition. Soil Dynamics and Earthquake Engineering. 56: 74–85. doi:10.1016/j.soildyn.2013.10.005.

Chang, W.-J. 2016. "Evaluation of liquefaction resistance for gravelly sands using gravel content–corrected shear-wave velocity." Journal of Geotechnical and Geoenvironmental Engineering 142(5): 04016002. https://doi.org/10.1061/(ASCE)GT.1943-5606.0001427

Chinese Design Code. 2001. Design code for building foundation of Chengdu region. Administration of Quality and Technology supervision of Sichuan Province PRC DB51/T5026-2001 [in Chinese].

Daniel, C., J. Howie, R. Campanella and A. Sy. 2004. Characterization of SPT grain size effects in gravels. Second international conference on site characterization (ISC’2).

Di Giulio, G., Cultrera, G., Cornou, C., Bard, P.Y. and Al Tfaily, B. 2021. Quality assessment for site characterization at seismic stations. Bulletin of Earthquake Engineering 19(12): 4643-4691. https://doi.org/10.1007/s10518-021-01137-6

Park, C. B., Miller, R. D., Xia, J. and Ivanov, J. 2007. Multichannel analysis of surface waves (MASW)- Active and passive methods. The Leading Edge 26: 60-64. https://doi.org/10.1190/1.2431832

Pollak, D., Gulam, V., Novosel, T., Avanić, R., Tomljenović, B., Hećej, N., Terzić, J., Stipčević, J., Bačić, M. and Kurečić, T. 2021. The preliminary inventory of coseismic ground failures related to December 2020 – January 2021 Petrinja earthquake series. Geologia Croatica: Journal of the Croatian Geological Survey and the Croatian Geological Society 74(2): 189-208. https://doi.org/10.4154/gc.2021.08

Rollins, K., J. Roy, S. Amoroso and N. Linton. 2021. Evaluation of the Dynamic Cone Penetration Test (DPT) for liquefaction triggering at gravel sites in Alaska and Italy. 6th International Conference on Geotechnical and Geophysical Site Characterization-ISC’6 Conference. https://doi.org/10.1061/(ASCE)GT.1943-5606.0002686

Rollins, K.M., Roy, J., Athanasopoulos-Zekkos, A., Zekkos,, D., Amoroso, S. and Cao, Z. 2021. A new dynamic cone penetration test–based procedure for liquefaction triggering assessment of gravelly soils. Journal of Geotechnical and Geoenvironmental Engineering 147(12): 04021141. https://doi.org/10.1061/(ASCE)GT.1943-5606.0002686

Rollins, K. M., J. Roy, A. Athanasopoulos-Zekkos, D. Zekkos, S. Amoroso, Z. Cao, G. Milana, M. Vassallo and G. Di Giulio. 2022. "A new V s-based liquefaction-triggering procedure for gravelly soils." Journal of Geotechnical and Geoenvironmental Engineering 148(6): 04022040. https://doi.org/10.1061/(ASCE)GT.1943-5606.0002784

Roy, J. and ROLLINS, K.M. (2022). “Effect of hydraulic conductivity and impeded drainage on the liquefaction potential of gravelly soils.” Canadian Geotechnical J., Canadian Science Publishing, 58(11) pp. 1950-1968, https://doi.org/10.1139/cgj-2021-0579

Seed, H. B. 1985. Influence of SPT Procedures in Soil Liquefaction Resistance Evaluations: ASCE Geotechnical Journal.

Šikić, K. 2014. Basic Geological Map of Republic Croatia 1:100.000, Bosanski Novi sheet. Croatian Geological Survey, Zagreb [in Croatian].

Tomljenović, B. and Csontos, L. 2001. Neogene–Quaternary structures in the border zone between Alps, Dinarides and Pannonian Basin (Hrvatsko zagorje and Karlovac Basins, Croatia). International Journal of Earth Sciences 90: 560–578. https://doi.org/10.1007/s005310000176

Uglešić, J. S., Skenderović, F., Lončar, I., Markušić, S. and Stanko, D. 2022. Regionally adjusted ground motion model: Case study of the M_L6.2 (M_w6.4) Petrinja (Croatia) 2020 earthquake. Stud. Geophys. Geod., 66 (2022), p. 162-186, DOI: 10.1007/s11200-022-0914-6

Ustaszewski, K., Kounov, A., Schmid, S.M., Schaltegger, U., Krenn, E., Frank, W. and Fügenschuh, B. 2010. Evolution of the Adria-Europe plate boundary in the northern Dinarides: From continent-continent collision to back-arc extension: Adria-Europe Plate Boundary, Dinarides. Tectonics 29. https://doi.org/10.1029/2010TC002668